Int. J. Heat Mass Transfer. Vol. 23, pp. 1303–1312
© Pergamon Press Ltd. 1980. Printed in Great Britain

0017-9310/80/1001-1303 $02.00/0

CONVECTION IN A ROTATING SPHERICAL ANNULUS WITH A UNIFORM AXIAL GRAVITATIONAL FIELD

R. J. DALLMAN* and R. W. DOUGLASS
Department of Mechanical Engineering, University of Nebraska, Lincoln, Nebraska 68588, U.S.A.

(*Received* 26 *August* 1979 *and in revised form* 25 *January* 1980)

Abstract—The steady combined convection of a Boussinesq fluid enclosed between two concentric rotating spheres is analytically investigated. The spheres rotate at constant rates and are maintained at uniform, but unequal temperatures. A uniform gravity field acts parallel to the rotation axis. The governing equations are solved using a partial spectral expansion method. This method provides solutions for Reynolds and Prandtl numbers significantly larger than currently available. The general nature of the flow field is shown to depend on the Reynolds number, the Prandtl number, and the Grashof number (presented in the ratio Gr/Re^2). Increasing any or all of these parameters causes enhanced convective heat transfer and an increase in the torque required to rotate the spheres. The secondary flow field is strongly dependent on the ratio Gr/Re^2, approaching the single-eddy pattern of natural convection as Gr/Re^2 becomes large.

NOMENCLATURE

$\hat{\mathbf{e}}$,	coordinate unit vector;
f_n,	angular momentum coefficient function;
$\mathbf{g}$,	gravitational force vector;
g_0,	gravitational acceleration constant;
Gr,	Grashof number, $g_0\beta(T_2 - T_1)R_2^3/\nu^2$;
h_n,	temperature coefficient function;
k,	thermal conductivity of the fluid;
M,	dimensionless torque;
M_0,	creeping flow dimensionless torque;
$P_n(\theta)$,	Legendre polynomial of the first kind of order n;
Pr,	Prandtl number, ν/α;
Q,	total heat transfer rate across the spheres;
Q_c,	total conduction heat transfer rate across the spheres;
r,	radial coordinate;
Ra,	Rayleigh number, $GrPr$;
Re,	Reynolds number, $\omega_0 R_2^2/\nu$;
T,	fluid temperature.

Greek symbols

α,	thermal diffusivity of the fluid;
β,	coefficient of volume expansion of the fluid;
ζ,	dimensionless temperature function;
ζ_c,	conduction temperature distribution;
η,	radius ratio of the spheres, R_1/R_2;
θ,	latitudinal coordinate;
μ,	viscosity of the fluid;
$\tilde{\mu}$,	angular velocity ratio of the spheres, ω_2/ω_1;
ν,	kinematic viscosity of the fluid;
π,	3.14159....;
ϕ,	longitudinal coordinate;
ψ,	stream function;
ω,	angular velocity of the fluid, $\Omega/(r^2 \sin^2\theta)$;
ω_0,	characteristic angular velocity of the spheres;
Ω,	angular momentum function;
∇^2,	Laplacian operator.

Superscripts

$(\ )'$,	dimensional or physical quantity.

Subscripts

$(\ )_1$,	inner sphere quantity;
$(\ )_2$,	outer sphere quantity;
$(\ )_r$,	radial component;
$(\ )_\theta$,	latitudinal component;
$(\ )_\phi$,	longitudinal component.

* Currently employed by: EG & G Idaho, Inc., Code Assessment Branch, P.O. Box 1625, Idaho Falls, Idaho 83401, U.S.A.

1. INTRODUCTION

COMBINED convection in rotating spherical annuli has recently been studied in a series of papers [1]–[4] dealing with uniform radial stratification of the fluid. In this paper, we present an approximate solution for combined convection in a rotating spherical annulus with the gravitational field parallel to the rotation axis. Although seemingly a minor change, the two problems are entirely different, being the same only in the forced convection limit. While the former configurations were applicable to some geophysical or meteorological situations, the present configuration models such physical flows as a rotating sphere viscometer [5] or a special purpose heat exchanger, either attractive for high pressure fluids. The interaction of the buoyancy and centrifugal forces also provides many interesting flow situations ranging from natural to forced convection.

Previous research concerning axially stratified spherical annulus flow can be divided into two groups: natural and combined convection flows. The problem has been approached both analytically and experimentally.

Photographic studies and measured temperature distributions in natural convection flows were first presented by Bishop *et al.* [6], [7] in which specific flow regimes were identified as dependent on the diameter ratio. Later experiments broadened these results to include diameter ratio studies and Grashof numbers ranging from 0.4 to 1.3×10^8 [8]–[10]. Nusselt–Grashof number correlations were also presented. Powe [11] has provided limits of relative gap width for which various Nusselt number correlations for spherical and cylindrical enclosures are applicable.

Mack and Hardee [12] studied the natural convection problem analytically by using a perturbation expansion in terms of powers of the Rayleigh number. Results included streamlines, velocity and temperature distributions, and the local and total surface heat transfer rates. Their Nusselt number dependence on the Rayleigh number compared with the earlier experimental correlations.

Combined convection flows were first studied by Riley [13] and Riley and Mack [14] by using a low order regular perturbation expansion in powers of the Reynolds number. The available flow regimes induced by the various rotation rates of the boundaries were studied and expressed in a flow map. Secondary flow contours were presented which showed the effects of increased stratification. Maximum values of the Reynolds numbers allowed were $O(1)$. To the order of solution presented, the total heat transfer rate was essentially that due to conduction.

Bestman [5] has presented a simplified analytical study of slow viscous convection in a concentric spherical viscometer. Only the primary flow was included in the analysis and was introduced in the dissipation terms of the energy equation. Body force effects were ignored. The intent was to provide a method to determine both a fluid's viscosity and thermal conductivity in one apparatus.

Experimental studies of combined convection were presented by Askin [15] and Maples *et al.* [16]. In these results only the inner sphere was allowed to rotate. Tabular and graphical results were presented for the Nusselt number dependence on the Grashof and Reynolds numbers. Reynolds numbers ranged upward from 3000.

In this paper, a broad range of combined convection flows in a rotating spherical annulus are studied analytically by using the method of partial spectral expansions. Valid solutions are found for Reynolds numbers up to two orders of magnitude larger than currently available. The effects of increasing Reynolds and Prandtl numbers, and buoyancy forces are individually studied. Results for the total heat transfer rate and rotational torque are also discussed.

2. GOVERNING EQUATIONS AND SOLUTION METHOD

A viscous Boussinesq fluid [17] fills a spherical annulus whose boundaries rotate at independent rates. Of principal importance is the orientation of the gravitational field, acting (uniformly) parallel to the rotation axis as $\mathbf{g} = g_0(-\cos\theta\,\hat{\mathbf{e}}_r + \sin\theta\,\hat{\mathbf{e}}_\theta)$. Unlike the earlier studies with uniform radial gravity [1]–[4], a subcritical flow (i.e. natural convection) can here be induced solely by the body forces if a temperature difference between the spheres exists.

Following Douglass *et al.* [1, 2], the equations governing the flow are written in terms of the stream function, $\psi(r,\theta)$, in a meridian plane representing the secondary flow, an angular momentum function, $\Omega(r,\theta)$, representing the primary flow, and a temperature function, $\zeta(r,\theta)$. The physical variables describing the flow are related to these dimensionless variables as

$$r' = R_2 r,$$

$$v'_r = R_2\omega_0\frac{\partial\psi/\partial\theta}{r^2\sin\theta}, \quad v'_\theta = -R_2\omega_0\frac{\partial\psi/\partial r}{r\sin\theta},$$

$$v'_\phi = R_2\omega_0\frac{\Omega}{r\sin\theta} = R_2\omega_0(r\sin\theta)\omega, \tag{1}$$

and

$$T' = (T_2 - T_1)\zeta + T_1,$$

where the nondimensionalization employed R_2, ω_0^{-1}, and $(T_2 - T_1)$ as the characteristic length, time, and temperature scales. Note that $\omega(r,\theta)$ is the fluid's angular velocity about the rotation axis and is related to $\Omega(r,\theta)$ as shown. The appropriate equations governing the steady flow are [18]:

$$D^2\Omega = \frac{Re}{r^2\sin\theta}\mathbf{J}\left(\frac{\Omega,\psi}{r,\theta}\right), \tag{2a}$$

$$\frac{1}{Re}D^4\psi = \frac{2}{r^3\sin^2\theta}\left[\Omega\,\mathbf{J}\left(\frac{\Omega, r\sin\theta}{r,\theta}\right) + D^2\psi\,\mathbf{J}\left(\frac{\psi, r\sin\theta}{r,\theta}\right)\right] + \frac{1}{r^2\sin\theta}\mathbf{J}\left(\frac{D^2\psi,\psi}{r,\theta}\right) - \frac{Gr}{Re^2}\sin\theta\,\mathbf{J}\left(\frac{r\cos\theta,\zeta}{r,\theta}\right), \tag{2b}$$

and

$$\nabla^2\zeta = \frac{RePr}{r^2\sin\theta}\mathbf{J}\left(\frac{\zeta,\psi}{r,\theta}\right), \tag{2c}$$

subject to (cf. [18]) the no slip condition at the rotating boundaries and uniform (but different) boundary temperatures. Here, $\mathbf{J}$ represents the Jacobian determinant, $D^2 = \partial^2/\partial r^2 + r^{-2}(\partial^2/\partial\theta^2 - \cot\theta\,\partial/\partial\theta)$, $D^4 = D^2(D^2)$. The solutions have, in general, only axisymmetry and exist in a domain $\eta \le r \le 1$, $0 \le \theta \le \pi$, and $0 \le \phi \le 2\pi$. The usual dimensionless groups characteristic of combined convection appropriately appear in the governing equations (2).

Since the governing system of equations is both coupled and non-linear, the method of partial spectral expansions was used to determine the spacial behavior of the dependent variables. This method has been extensively studied by Orszag and his associates (for example, [19]) and has previously been applied to viscous flows (e.g. [20]) and to heat transfer problems (e.g. [1]–[3], [21]). The general application of the method is outlined in [21] and a detailed discussion of its use in the present problem is given in [18]. The advantage of this method over perturbation expansion methods is that solutions can be found for larger values of Re, Pr, and Gr/Re^2. In some cases solutions can be found which approach hydrodynamic instability [20].

3. RESULTS AND DISCUSSION

The flow in a heated rotating spherical annulus is a complicated composite of the primary and secondary flow which, in turn, is linked to the temperature distribution. Of course, the latter is determined in part by the boundary temperatures. The primary flow (Ω or ω) is established by the rotation of the boundaries while the secondary flow (ψ) has its origin in two different mechanisms. One is the centrifugal acceleration of the fluid generated by the primary flow and the other is the buoyancy force caused by density variations due to non-uniform temperatures in the fluid. In the first extreme (i.e. given by either isothermal flow or forced convection) the flow pattern is well established as being both axially and equatorially symmetric (e.g. [1] and [20]). The opposite extreme of natural convection in spherical annuli has only axisymmetry (with no azimuthal primary flow) and is equally well studied as indicated in the Introduction. It is, therefore, reasonable that these two mechanisms will combine to form flows characteristic of both extremes.

The appropriate index of the relative importance of these mechanisms is Gr/Re^2 and is seen to multiply the body force term of equation (2b). If $Gr/Re^2 \to 0$, the dominant mechanism is centrifugal acceleration and the flow is said to be forced convection. Likewise, if $Gr/Re^2 \to \infty$, the flow is body force dominated. Intermediate values ($Gr/Re^2 = 0(1)$) show both sorts of convection. Dallman [18] has proved that it is unnecessary to consider both positive and negative values of Gr/Re^2 since the flow field in one case is a simple rotation of the other with no net change.

There are four other dimensionless groups which appear in the equations of motion and boundary conditions. These are the Reynolds (Re) and Prandtl (Pr) numbers and the radius ($\eta = R_1/R_2$) and angular velocity ($\tilde{\mu} = \omega_2/\omega_1$) ratios. Re may be thought of as a primary flow parameter, Pr as a fluid property index, and η and $\tilde{\mu}$ as boundary condition parameters. Of major interest here is the effect on the flow of increasing Re, Pr and Gr/Re^2. In order to limit the discussion to these effects, η will be maintained at 0.5 while only two values of $\tilde{\mu}$ will be used. The general nature of η and $\tilde{\mu}$ effects are given in [4] and [14]. Because of the axial symmetry, the flow field need only be shown in a representative meridian plane.

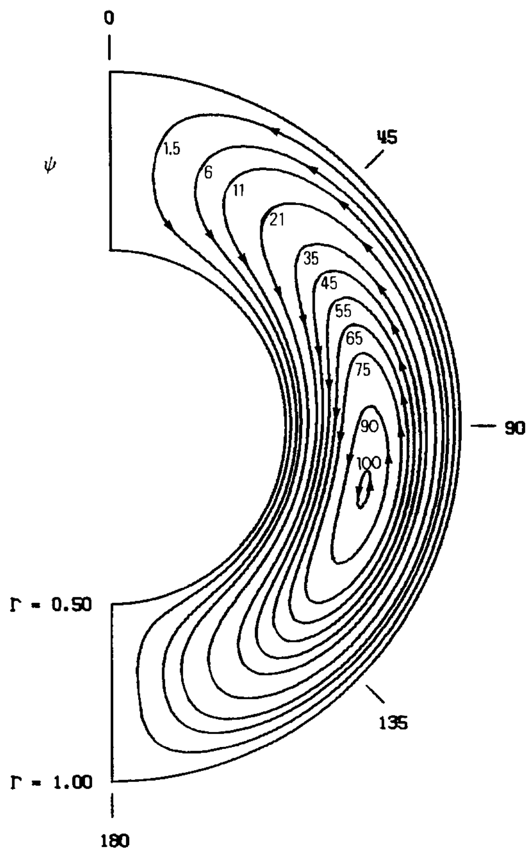

FIG. 1. Secondary flow for $Re = 50$ and with $\tilde{\mu} = 2$, $\eta = 0.5$, $Re = \omega_2 R_2^2/\nu$, $Gr/Re^2 = 1$ and $Pr = 1$. Values shown are $10^4 \times -\psi$.

Reynolds number effects

The first effect to be discussed is that of increasing Re (for $\eta = 0.5$, $\tilde{\mu} = 2$, $Gr/Re^2 = 1$ and $Pr = 1$). Figure 1 shows streamlines for a Reynolds number of 50. Clearly, the characteristic 'kidney' shaped eddy of natural convection is present [6, 7]; however, the centrifugal accelerations due to rotation result in an enhanced counterclockwise circulation. For larger values of Re this effect continues, increasing nearly linearly with Re. Regions of up- and down-drafts are also increasingly concentrated near the solid boundaries as Re increases. The low Reynolds number circulation result compares favorably with that of Riley and Mack [13, 14]. There is little distortion of the streamlines in any of these moderate Re cases.

Figure 2 shows isotherms for the same parameters as Fig. 1. The basic nature of low Re isotherms consists of lines of constant ζ which are almost concentric circles, varying little from the conduction solution: $\zeta_c(r) = (1 - \eta/r)/(1 - \eta)$. As Re is increased to 50 (Fig. 2), the isotherms are pushed slightly toward the outer sphere in the southern hemisphere and toward the inner sphere in the northern. This trend significantly increases as Re increases. Such behavior is explained in terms of the secondary flow results of Fig. 1. For Gr positive, the outer sphere is warmer than the inner sphere. As cool fluid is swept upward from its coldest

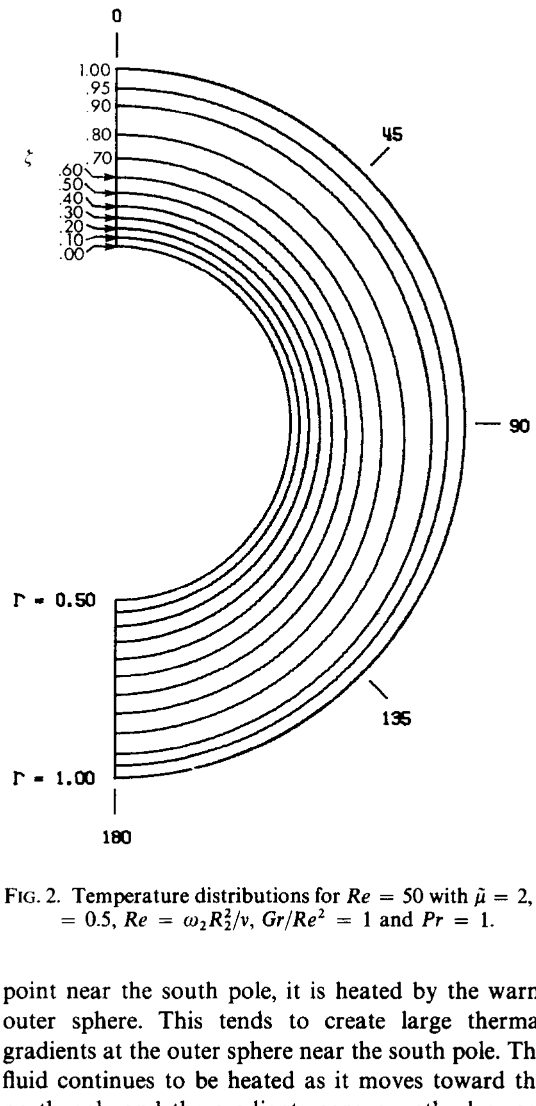

FIG. 2. Temperature distributions for $Re = 50$ with $\tilde{\mu} = 2$, $\eta = 0.5$, $Re = \omega_2 R_2^2/\nu$, $Gr/Re^2 = 1$ and $Pr = 1$.

point near the south pole, it is heated by the warm outer sphere. This tends to create large thermal gradients at the outer sphere near the south pole. The fluid continues to be heated as it moves toward the north pole and the gradients consequently decrease until a minimum is reached at the north pole. In a region near the north pole then, a relatively large volume of warm fluid is established. This is reflected in the isotherms being more concentrated near the inner sphere. A cooling sequence identical to that for the outer sphere occurs as the warm fluid sweeps along the cool inner sphere which ultimately causes a relatively large area of cool fluid near the south pole to develop.

The fluid's angular velocity distribution is shown in Fig. 3 for the same set of parameters. The small *Re* results again show a characteristic concentric circle distribution. As *Re* is increased, these contours become dramatically distorted; in some cases the fluid rotates faster than the boundaries. Although seeming at first to be incorrect, this behaviour can be shown to be possible by referring to the isotherms of Fig. 2 and recalling conservation of angular momentum. From Fig. 2 it is seen that as *Re* increases, relatively larger regions of warm and cool fluid form near the north and south poles, respectively, as compared to the low *Re* results. This demands that the cooler, more dense fluid rotate slower than the comparable forced convection flow. The warmer, less dense fluid must likewise rotate faster, in some cases exceeding the angular speed of the boundaries. For the $Re = 100$ case, the light fluid is moving over 117% the speed of the outer surface and the slow moving cool fluid interacting with the warm fluid forms a nearly horizontal equatorial shear layer. A distinct boundary layer also develops along the inner sphere. Experimental verification of these results is not available in the literature to the authors' knowledge.

Prandtl number effects

The second parameter to be studied is the Prandtl number, $Pr = \nu/\alpha$. All other flow parameters are held at $\eta = 0.5$, $\tilde{\mu} = 2$, $Re = 50$, and $Gr/Re^2 = 1$. Trends are adequately shown by illustrating two values: $Pr = 1$ and $Pr = 10$. The flow fields for $Pr = 1$ have been shown in Figs. 1 for ψ, 2 for ζ and 3(a) for ω.

Since the Prandtl number is concerned with fluid properties only, changing *Pr* can be thought of as altering the working fluid, say, from air to water. A large value of *Pr* implies that the fluid is relatively more able to diffuse momentum than energy, thus velocity gradients will be relatively small and thermal gradients large. For small values ($Pr < 1$), the reverse is true. $Pr = 1$ implies that these gradients are of the same magnitude.

This behavior is borne out by comparing the isotherms shown in Fig. 4(a) for $Pr = 10$ with those of Fig. 2. For the large Prandtl number flow, a region of very cool fluid fills a large portion of the southern hemisphere forming a thermal boundary layer along the southern part of the warm outer sphere. A less pronounced large region of warm fluid occupies the northern hemisphere with a thermal boundary layer along the northern inner sphere. Again, these segregated regions are only slightly established for $Pr = 1$. In each case, the secondary flow causes the fluid to be swept upward along the warm outer sphere and downward along the cool inner sphere. As it does, the larger *Pr* is more resistant to changing its temperature, causing large warm and cool regions to persist in the annulus.

This phenomenon has implications principally for the secondary flows. Once a significant segregation of fluid has been established, the warm fluid near the north pole and the cool fluid near the south pole are increasingly resistant to being moved from their stable alignment with the gravitational field. Thus, the secondary flow circulation of Fig. 1 for $Pr = 1$ is significantly retarded as shown in Fig. 4(b) for $Pr = 10$. It remains undistorted, however, The primary flow, ω, is not significantly different from that for $Pr = 1$. This is not an unexpected result since the enhanced thermal segregation of the fluid for increasing *Pr* does not directly influence ω (or Ω) in the governing equations (cf. equation 2(a)). The basic explanation for the curious behavior of ω, however, remains unchanged.

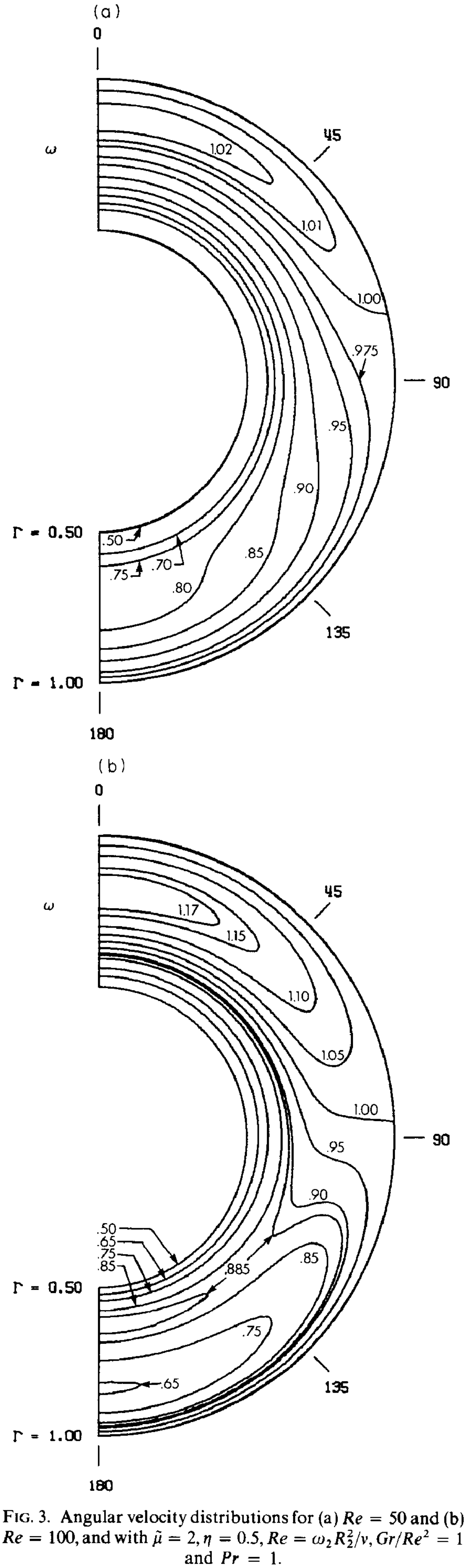

FIG. 3. Angular velocity distributions for (a) $Re = 50$ and (b) $Re = 100$, and with $\tilde{\mu} = 2$, $\eta = 0.5$, $Re = \omega_2 R_2^2/\nu$, $Gr/Re^2 = 1$ and $Pr = 1$.

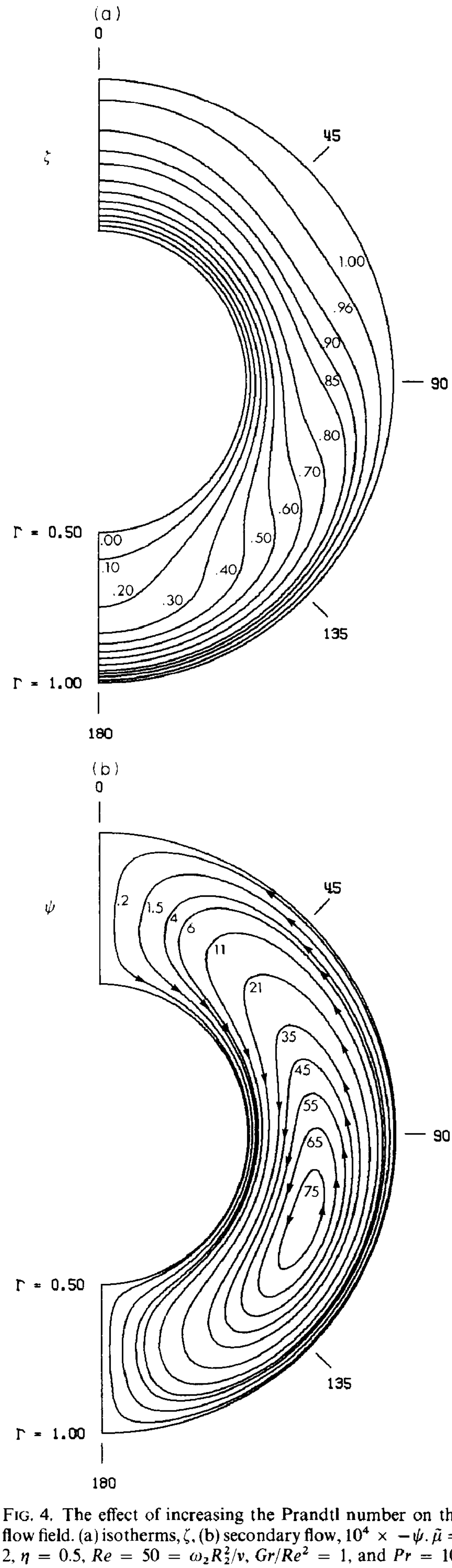

FIG. 4. The effect of increasing the Prandtl number on the flow field. (a) isotherms, ζ, (b) secondary flow, $10^4 \times -\psi$. $\tilde{\mu} = 2$, $\eta = 0.5$, $Re = 50 = \omega_2 R_2^2/\nu$, $Gr/Re^2 = 1$, and $Pr = 10$.

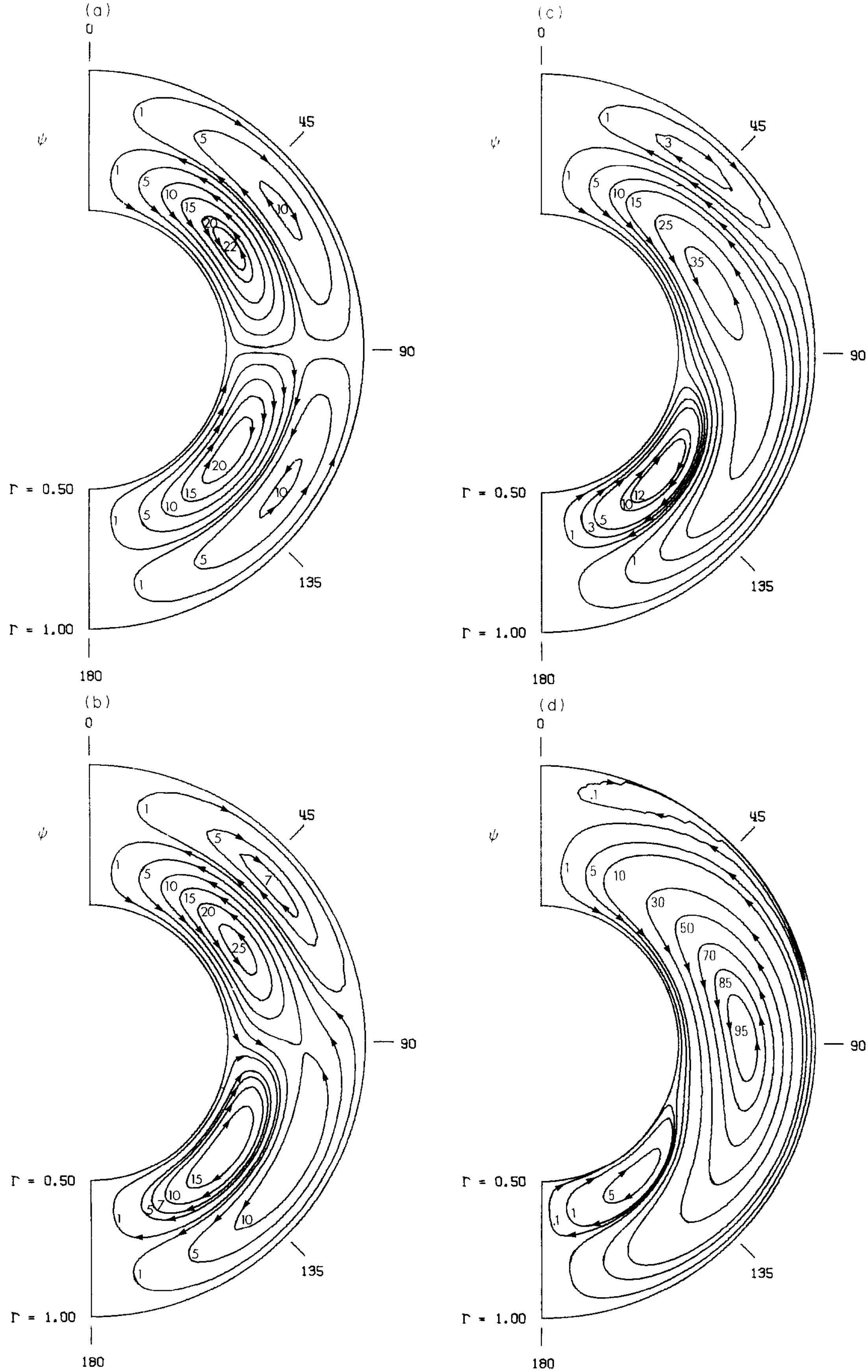

FIG. 5. The secondary flow field as influenced in increasing buoyancy forces for $\tilde{\mu} = -1/3$, $\eta = 0.5$, $Re = 50 = \omega_2 R_2^2/\nu$, and $Pr = 1$. (a) $Gr/Re^2 = 0$, (b) $Gr/Re^2 = 1/10$, (c) $Gr/Re^2 = 1/3$ and (d) $Gr/Re^2 = 1$. Values shown are $10^4 \times \psi$.

Gr/Re^2 *effects*

The final series of results illustrate the relative effect of increasing gravitational forces as characterized by Gr/Re^2. These results are presented for $\eta = 0.5$, $\tilde{\mu} = \omega_2/\omega_3 = -1/3$, $Pr = 1$ and $Re = 50$. $\tilde{\mu} = -1/3$ implies that the inner sphere is rotating three times as fast as the outer sphere and in the opposite direction. These results are perhaps most interesting since the competition between the centrifugal accelerations and buoyancy forces is vividly seen.

First the results for the secondary flows are discussed (Fig. 5). In Fig. 5(a) $Gr/Re^2 = 0$, implying that buoyancy forces are zero. The flow is then entirely responsive to the centrifugal acceleration of the fluid. This flow has equatorial symmetry. In the northern latitudes, two eddies are observed, one near the inner sphere with a counterclockwise circulation and one along the outer surface with clockwise circulation. For this particular value of $\tilde{\mu}$, an additional competition aside from that between centrifugal and buoyancy forces exists in that the centrifugally driven secondary flow established by the inner sphere is not sufficient to dominate that of the outer sphere, and vice versa. Thus, both are manifest within the annulus. In Fig. 5(b), a slight buoyancy force has been introduced to the fluid. Already, the secondary flow has been altered with equatorial symmetry abolished through communication between the two counterclockwise eddies. This direction of circulation is preferred and encouraged by the gravitational field. As the buoyancy forces are increased through $Gr/Re^2 = 1/3$ to 1 [Fig. 5(c) and (d)], the counterclockwise eddies are totally merged and enhanced while the two clockwise eddies are reduced in size and magnitude. Even for $Gr/Re^2 = 1$, the centrifugally driven eddies are not obscured indicating both driving mechanisms still exist. These results are qualitatively the same as those in [14] for $Re = 3$.

For this set of flow parameters, the isotherms and angular velocity contours remain nearly unaltered from their characteristic forced convection, concentric circular pattern. The interested reader may refer to [18] for these results.

Net heat transfer rate and moment acting on the spheres

Of particular interest is the overall considerations of heat transfer and torque. These will be of importance in thermal design applications since for each net heat exchange rate, power (i.e. torque) will need to be supplied in order to keep the spheres in motion. Each quantity is found by the integration of a gradient over the surface of a sphere, and is seen to depend on all of the flow parameters.

Consider first the net rate of heat transfer across a solid spherical surface defined as

$$Q = \frac{Q'}{kR_2(T_2 - T_1)} = 2\pi \int_{\theta=0}^{\pi} \times \sin\theta \left[r^2 \frac{\partial \zeta}{\partial r} \right]_{\eta,1} \mathrm{d}\theta = 4\pi \left(r^2 \frac{\mathrm{d}h_0}{\mathrm{d}r} \right)_{\eta,1}, \quad (3)$$

where $h_0(r)$ is the first coefficient in the spectral expansion for temperature (cf. [18]). The total rate of heat transfer for conduction only is used to normalize Q' giving

$$\frac{Q}{Q_c} = \frac{(1-\eta)}{\eta} \left(r^2 \frac{\mathrm{d}h_0}{\mathrm{d}r} \right)_{\eta,1}, \quad (4)$$

where

$$Q_c' = \frac{4\pi\eta}{(1-\eta)} [R_2 k(T_2 - T_1)]. \quad (5)$$

In steady flows, the net rate of heat transfer across each sphere must be the same, since dissipation has been neglected.

From the energy equation (2c) the mechanism for convection is observed to be only the stream function. This must be so in the assumed axially symmetric flow. Thus, the explanation of the behavior of Q/Q_c as it depends on the flow parameters is linked to that of ψ. Specifically, the size of the convective energy terms (involving ζ and ψ) is indicated by the product $RePr$. Referring to Figs. 1 and 4, the magnitude of the secondary circulation generally increases with Re and Pr. It is reasonable to suppose, then, that Q/Q_c will as well. This behavior is borne out by the typical results of Fig. 6 (solid lines). Here the dependence of Q/Q_c on Re and Pr is given for $Gr/Re^2 = 1$, $\tilde{\mu} = 2$, and $\eta = 0.5$.

In Fig. 7, the large Re (>3000) experimental results for $\tilde{\mu} = 0$ (only the inner sphere rotating), $\eta = 0.5$ and $Pr = 0.72$ as reported by Maples *et al.* [16] are compared to the current intermediate values of $Re = 100$ for $Pr = 1$. The experimental data were presented in tabular (and graphical) form in [16] as Nusselt numbers (Nu here appropriately converted to Q/Q_c) for given Grashof and Reynolds numbers with four values of Nu in each set of Re data. The Reynolds numbers were nearly constant for each run with a maximum deviation of less than 10%. Grashof numbers were varied widely within each set. Curves shown in Fig. 7, then, present results for average Reynolds numbers ($\bar{R}e$) for each set of data in [16]. While the hydrodynamic stability of the experimental combined convection flows is not known, it is at least probable that the flow field has characteristics of turbulence based on the viscous flow data of Munson *et al.* [22, 23] who have shown that the viscous flow is unstable for $Re \gtrsim 1300$. The current data found here are for laminar flows. As $Gr/Re^2 \rightarrow 0$, the forced convection minima of Q/Qc are approached. There is a tendency in each case presented for the total rate of heat transfer to increase with increasing buoyancy forces. The principal reasons for this behavior are that the secondary flow circulation in combined convection is generally

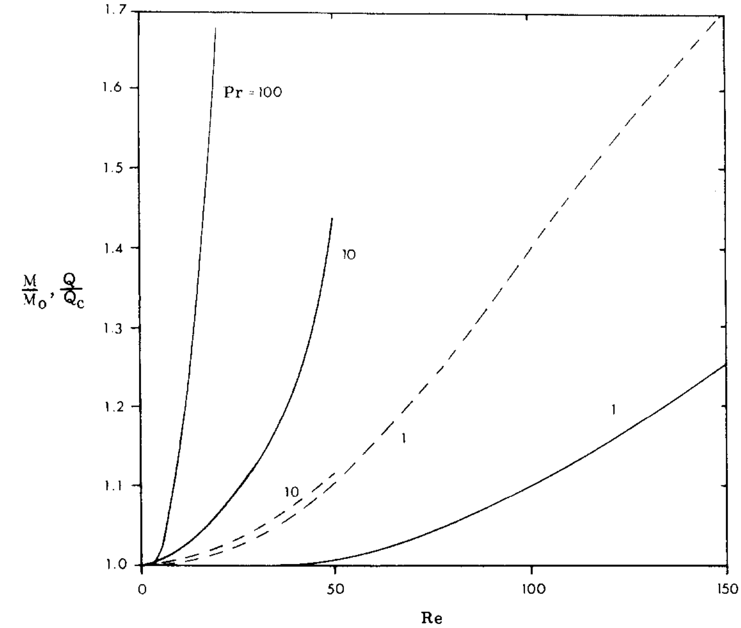

FIG. 6. The effect of increasing Re and Pr on the total heat transfer rate (solid lines) and on the torque required to rotate the spheres (dashed lines) for $\tilde{\mu} = 2$, $\eta = 0.5$, and $Gr/Re^2 = 1$.

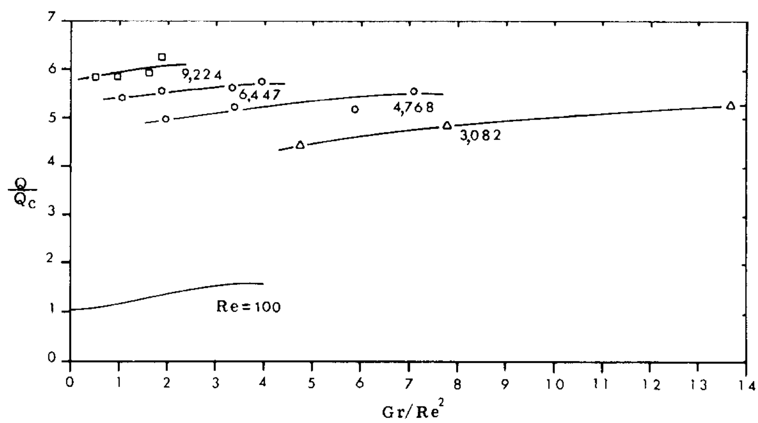

FIG. 7. Combined convection total heat transfer rates for $\tilde{\mu} = 0$, $\eta = 0.5$, and $Pr = 1$ for the current results and $Pr = 0.72$ for the large Re experimental data [16].

stronger than in forced convection and that a single eddy usually sweeps past the entire spherical surface in combined flows in contrast to the equatorially symmetric eddy pattern in forced flows. This phenomenon is in contradiction to the usual external flow situation where heat transfer is enhanced by an increasing degree of forced convection as reported by Yuge [24], for example, for mixed convection due to a single rotating sphere in air.

The final quantity to be discussed is the torque required to rotate the spheres defined as:

$$M = \frac{M'}{\mu R_2^3 \omega_0} = 2\pi \int_{\theta=0}^{\pi} \sin\theta \left[r^4 \frac{\partial}{\partial r}\left(\frac{\Omega}{r^2}\right)\right]_{\eta,1} d\theta$$
$$= \frac{8}{3}\pi \left[r^2 \left(\frac{d}{dr}\left(f_0 - \frac{1}{5} f_2 \right) - \frac{2}{r}\left(f_0 - \frac{1}{5} f_2 \right)\right)\right]_{\eta,1} = \frac{8}{3}\pi m, \quad (6)$$

where f_0 and f_2 are the first two coefficients in the spectral expansion for Ω (cf. [18]). As for the total heat transfer rate, the total moment is normalized. Here, this quantity is the creeping flow torque, M_0', representing the torque in the absence of any secondary flow, defined as

$$M_0' = 8\pi\mu R_2^3 \frac{(\omega_2 - \omega_1)}{(1-\eta^3)} \eta^3 \quad (7)$$

giving

$$\frac{M}{M_0} = \frac{(1-\eta^3)\omega_0}{3\eta^3(\omega_2 - \omega_1)} m_{\eta,1}. \quad (8)$$

Again, the magnitude of the torque required to rotate each sphere must be identical in steady state flow.

Typical results for the dependence of the torque on both Re and Pr are shown in Fig. 6 (dashed lines) for $\tilde{\mu} = 2$, $\eta = 0.5$, and $Gr/Re^2 = 1$. Note that the general behavior of both Q/Q_c and M/M_0 is similar. Of most

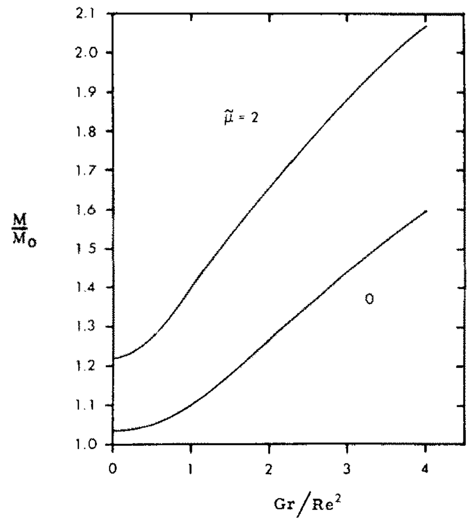

FIG. 8. Combined convection effects on the moment acting on the spheres for $\tilde{\mu} = 0$ and $2, \eta = 0.5, Re = 100$, and $Pr = 1$.

significance is the result showing the relative insensitivity of the torque to increasing Pr. By referring to equation (2a), however, the primary flow, hence the moment, does not directly depend on Pr as the heat transfer results do. Only through the changes in ψ induced by the energy equation (2c), are Pr effects introduced to the angular momentum equation (2a).

The effect of increasing buoyancy forces on the moment are shown in Fig. 8. Since Gr/Re^2 directly influences ψ in equation (2b) and thus Ω in equation (2a), an altered secondary flow will cause distortions in the primary flow yielding the net effect of increasing M/M_0. Experimentally measured moments for combined convection flows are as yet unavailable in the literature.

4. CONCLUSION

Approximate solutions for the steady combined convection in a rotating spherical annulus have been found and discussed for Reynolds and Prandtl numbers much larger than currently in the literature. A gravitational field parallel to the rotation axis provides the driving force for buoyancy effects when the spheres are maintained at different temperatures. The flow is assumed to be axisymmetric, and thus is a function of only the radial and meridianal coordinates.

Five parameters which arise from the nondimensionalization affect the flow. The radius ratio, $\eta = R_1/R_2$, was fixed at a value of 0.5, a compromise between narrow-gap and wide-gap geometries. The angular velocity ratio, $\tilde{\mu} = \omega_2/\omega_1$, affects the nature of the secondary flow field for small Grashof numbers. Negative values of $\tilde{\mu}$ may cause double-eddy patterns, while positive values result in single-eddy patterns. Increasing the Reynolds number enhances the secondary flow circulation by increasing centrifugal forces, and tends to improve heat transfer. The Grashof number is an indicator of the importance of buoyancy forces and appears in the ratio Gr/Re^2. Changing the sign of Gr has the effect of rotating the flow pattern (ψ, ω and ζ) 180° and changing the sign of ψ. For $Gr > 0$, increasing Gr/Re^2 causes negative (counterclockwise) eddies to be enhanced and positive (clockwise) eddies to be retarded. In both cases, as $|Gr/Re^2| \to \infty$, the flow approaches that for natural convection, and heat transfer is improved. Increasing the Prandtl number results in a slightly retarded secondary flow, and causes locally larger temperature gradients. This results in larger total heat transfer rates. The torque required to rotate the spheres also increases with increasing Re, Gr/Re^2, and Pr.

Acknowledgement—The authors would like to express their thanks to Mr Jim Nelson who developed and perfected the time-saving plotting routines used in drawing the annular flow field data.

REFERENCES

1. R. Douglass, B. Munson and E. Shaughnessy, Thermal convection in rotating spherical annuli—1. Forced convection, *Int. J. Heat Mass Transfer* **21**, 1543–1553 (1978).
2. R. Douglass, B. Munson and E. Shaughnessy, Thermal convection in rotating spherical annuli—2. Stratified flows, *Int. J. Heat Mass Transfer* **21**, 1555–1564 (1978).
3. E. Shaughnessy and R. Douglass, The effect of stable stratification on the motion in a rotating spherical annulus, *Int. J. Heat Mass Transfer* **21**, 1251–1259 (1978).
4. R. Douglass, E. Shaughnessy and B. Munson, Small Reynolds number combined convection in rotating spherical annuli, *J. Heat Transfer* in press (1979).
5. A. Bestman, Heat transfer in the biconical and concentric spherical viscometer, *J. Heat Transfer* **100**, 750–752 (1978).
6. E. Bishop, R. Kolflat, L. Mack and J. Scanlan, Convective heat transfer between concentric spheres, *Proc. 1964 Heat Transf. Fluid Mech. Inst.*, pp. 69–80, Stanford University Press, Palo Alto (1964).
7. E. Bishop, R. Kolflat, L. Mack and J. Scanlon, Photographic studies of convection patterns between concentric spheres, *Soc. Photo-optical Instrum. Engrs J.* **3**, 47–49 (1964).
8. E. Bishop, L. Mack and J. Scanlan, Heat transfer by natural convection between concentric spheres, *Int. J. Heat Mass Transfer* **9**, 649–662 (1966).
9. J. Scanlan, E. Bishop and R. Powe, Natural convection heat transfer between concentric spheres, *Int. J. Heat Mass Transfer* **13**, 1857–1872 (1970).
10. S. Yin, R. Powe, J. Scanlon and E. Bishop, Natural convection flow patterns in spherical annuli, *Int. J. Heat Mass Transfer* **16**, 1985–1795 (1973).
11. R. Powe, Bounding effects on the heat loss by free convection from spheres and cylinders, *J. Heat Transfer* **96**, 558–560 (1974).
12. L. Mack and H. Hardee, Natural convection between concentric spheres at low Rayleigh numbers, *Int. J. Heat Mass Transfer* **11**, 387–396 (1968).
13. T. Riley, Thermal influence on the slow viscous flow of a fluid between rotating concentric spheres, Ph.D. Thesis, Univ. of Texas, Austin, Texas (1971).
14. T. Riley and L. Mack, Thermal effects on slow viscous flow between rotating concentric spheres, *Int. J. Nonlinear Mech.* **7**, 275–288 (1972).
15. K. Askin, Convective heat transfer from a rotating inner sphere to a stationary outer sphere, M.S. Thesis, Auburn Univ., Auburn, Alabama (1971).
16. G. Maples, D. Dyer, K. Askin and D. Maples, Convective heat transfer from a rotating inner sphere to a stationary outer sphere, *J. Heat Transfer* **95**, 546–547 (1973).
17. D. Gray and A. Giorgini, The validity of the Boussinesq

approximation for liquids and gases, *Int. J. Heat Mass Transfer* **19,** 545–551 (1976).
18. R. Dallman, Combined convection in a rotating spherical annulus, M.S. Thesis, Univ. of Nebraska, Lincoln, Nebraska (1978).
19. D. Gottlieb and S. Orszag, Numerical analysis of spectral methods: Theory and applications, CBMS-NSF Regional Conf. Series in Applied Mathematics, 26, Soc. for Industrial and Applied Math., Philadelphia, Pennsylvania (1977).
20. B. Munson and D. Joseph, Viscous incompressible flow between concentric rotating spheres—1. Basic flow, *J. Fluid Mech.* **49,** 289–303 (1971).
21. E. Shaughnessy, J. Custer and R. Douglass, Partial spectral expansions for problems in thermal convection, *J. Heat Transfer* **100,** 435–441 (1978).
22. B. Munson and D. Joseph, Viscous incompressible flow between concentric rotating spheres—2. Hydrodynamic stability, *J. Fluid Mech.* **49,** 305–318 (1971).
23. B. Munson and M. Menguturk, Viscous incompressible flow between concentric rotating spheres—3. Linear stability and experiments, *J. Fluid Mech.* **69,** 705–719 (1975).
24. T. Yuge, Experiments on heat transfer from spheres including combined natural and forced convection, *J. Heat Transfer* **82,** 215–220 (1960).

CONVECTION DANS UN ESPACE ANNULAIRE SPHERIQUE TOURNANT DANS UN CHAMP GRAVITATIONNEL AXIAL ET UNIFORME

Résumé—On étudie la convection stationnaire d'un fluide de Boussinesq entre deux sphères concentriques qui, tournant à des vitesses égales et constantes, sont maintenues à des températures uniformes mais inégales. Un champ uniforme de pesanteur agit parallèlement à l'axe de rotation. Les équations sont résolues en utilisant une méthode de développement spectral partiel. Cette méthode donne des solutions pour des nombres de Reynolds et de Prandtl plus éléves que de coutume.

La nature générale du champ d'écoulement dépend des nombres de Reynolds, de Prandtl et de Grashof (présent dans le rapport Gr/Re^2). Un accroissement d'un quelconque de ces paramètres provoque une augmentation du transfert thermique et un accroissement du couple nécessaire pour faire tourner les sphères. L'écoulement secondaire est fortement dépendant du rapport Gr/Re^2 et il approche la configuration de convection naturelle à un seul tourbillon quand Gr/Re^2 devient grand.

KONVEKTION IN EINEM ROTIERENDEN SPHÄRISCHEN RINGRAUM MIT EINEM GLEICHFÖRMIGEN AXIALEN GRAVITATIONSFELD

Zusammenfassung—Es wird die stationäre, gemischte Konvektion eines Boussinesq-Fluids, das zwischen zwei konzentrischen, rotierenden Kugelschalen eingeschlossen ist, analytisch untersucht. Die Kugelschalen rotieren mit konstanten Geschwindigkeiten und werden auf gleichförmigen, aber unterschiedlichen Temperaturen gehalten. Parallel zur Rotationsachse wirkt ein Gravitationsfeld. Die Bestimmungsgleichungen werden mittels einer partiellen, spektralen Reihenentwicklung gelöst. Diese Methode liefert Lösungen für bedeutend größere als die gegenwärtig erreichbaren Reynolds- und Prandtl-Zahlen. Die allgemeine Beschaffenheit des Strömungsfeldes erweist sich als abhängig von der Reynolds-Zahl, der Prandtl-Zahl und der Grashof-Zahl (dargestellt in Abhängigkeit vom Verhältnis Gr/Re^2). Die Vergrößerung einzelner oder aller Parameter bewirkt erhöhten konvektiven Wärmeübergang und eine Zunahme des für die Rotation der Kugelschalen erforderlichen Drehmoments. Das sekundäre Strömungsfeld ist stark von dem Verhältnis Gr/Re^2 abhängig und nähert sich dem Einzelwirbel-Muster der freien Konvektion, wenn Gr/Re^2 groß wird.

КОНВЕКЦИЯ ВО ВРАЩАЮЩЕМСЯ СФЕРИЧЕСКОМ КОЛЬЦЕВОМ ЗАЗОРЕ ПРИ НАЛИЧИИ ОДНОРОДНОГО ОСЕВОГО ГРАВИТАЦИОННОГО ПОЛЯ

Аннотация — В приближении Буссинеска аналитически исследуется стационарная комбинированная конвекция в жидкости, помещенной между двумя концентрическими сферами, вращающимися с постоянной скоростью и имеющими постоянную, но разную температуру. Однородное поле тяжести направлено параллельно оси вращения. Основные уравнения решаются с помощью метода спектрального разложения. Этот метод позволяет получать решения для значений чисел Рейнольдса и Прандтля, намного превышающих те, которые исследовались до настоящего времени.

Показано, что общий характер течения зависит от числа Рейнольдса, числа Прандтля и числа Грасгофа (представленных отношением Gr/Re^2). Рост любого из этих параметров вызывает интенсификацию конвективного теплопереноса и увеличение момента вращения сфер. Картина вторичного течения сильно зависит от отношения Gr/Re^2 и с его увеличением стремится к структуре естественноконвективного течения с единичным вихрем.